

Thioether-Triphenolate Bimetallic Iron(III) Complexes as Robust and Highly Efficient Catalysts for Cycloaddition of Carbon Dioxide to Epoxides

*Antonio Buonerba,^{ab} Francesco Della Monica,^a Assunta De Nisi,^c Ermanno Luciano,^a Stefano Milione,^{ab} Alfonso Grassi,^{ab} Carmine Capacchione^{*ab} and Bernhard Rieger^d*

^a Dipartimento di Chimica e Biologia, Università degli Studi di Salerno, via Giovanni Paolo II 132, 84084 Fisciano (SA), Italy.

^b CIRCC, Interuniversity Consortium Chemical Reactivity and Catalysis, Via Celso Ulpiani 27, 70126 Bari, Italy

^c Dipartimento di Chimica G. Ciamician, Alma Mater Studiorum, Università di Bologna, via Selmi 2, Bologna, Italy

^d WACKER Lehrstuhl für Makromolekulare Chemie, Technische Universität München, Lichtenbergstrasse 4, 85748 Garching, Germany.

* *E-mail:* ccapacchione@unisa.it

Table of Contents

NMR Characterization.....	1
Figure S1. ^1H NMR spectrum of the pro-ligand L_H (CD_2Cl_2 , 400 MHz).....	1
Figure S2. ^{13}C NMR spectrum of the pro-ligand L_H (CD_2Cl_2 , 250 MHz).....	2
Figure S3. ^1H NMR spectrum of the pro-ligand L_{Cum} (CD_2Cl_2 , 400 MHz).....	3
Figure S4. ^{13}C NMR spectrum of the pro-ligand L_{Cum} (CD_2Cl_2 , 400 MHz).....	4
ESI-MS Characterization.....	5
Figure S5. Mass spectrum of the pro-ligand L_H (acetonitrile as solvent).....	5
Figure S6. Mass spectrum of the complex C_H (acetonitrile as solvent).....	6
Figure S7. Mass spectrum of the pro-ligand L_{Cum} (acetonitrile as solvent).....	7
Figure S8. Mass spectrum of the complex C_{Cum} (acetonitrile as solvent)	8
FT-IR Characterization.....	9
Figure S9. FT-IR spectrum of the pro-ligand L_H (KBr disk).....	9
Figure S10. FT-IR spectrum of the complex C_H (KBr disk).....	10
Figure S11. Comparison of the FT-IR spectra of the pro-ligand L_H (blue curve) and of the iron(III) complex C_H (red curve).....	11
Figure S12. Magnification of the region $1450\text{-}1415\text{ cm}^{-1}$ (for the $\text{CH}_2\text{-S-C}$ deformation) ^{1,2} of the FT-IR spectra of the pro-ligand L_H (blue curve) and of the iron(III) complex C_H (red curve).....	12
Figure S13. Magnification of the region $1270\text{-}1220\text{ cm}^{-1}$ (for the $\text{CH}_2\text{-S-C}$ wagging) ^{1,2} of the FT-IR spectra of the pro-ligand L_H (blue curve) and of the iron(III) complex C_H (red curve).....	13
Figure S14. Magnification of the region $680\text{-}600\text{ cm}^{-1}$ (for the C-S stretching vibration) ^{1,2} of the FT-IR spectra of the pro-ligand L_H (blue curve) and of the iron(III) complex C_H (red curve).....	14
Figure S15. FT-IR spectrum of the pro-ligand L_{Cum} (KBr disk)	15
Figure S16. FT-IR spectrum of the complex C_{Cum} (KBr disk)	16
Figure S17. Comparison of the FT-IR spectra of the pro-ligand L_{Cum} (blue curve) and of the iron(III) complex C_{Cum} (red curve).....	17

Electronic Supplementary Information

Figure S18. Magnification of the region 1450-1415 cm ⁻¹ (for the CH ₂ -S-C deformation) ^{1,2} of the FT-IR spectra of the pro-ligand L_{Cum} (blue curve) and of the iron(III) complex C_{Cum} (red curve).....	18
Figure S19. Magnification of the region 1270-1220 cm ⁻¹ (for the CH ₂ -S-C wagging) ^{1,2} of the FT-IR spectra of the pro-ligand L_{Cum} (blue curve) and of the iron(III) complex C_{Cum} (red curve).....	19
Figure S20. Magnification of the region 680-600 cm ⁻¹ (for the C-S stretching vibration) ^{1,2} of the FT-IR spectra of the pro-ligand L_{Cum} (blue curve) and of the iron(III) complex C_{Cum} (red curve).....	20
UV-Vis Analysis.	21
Figure S21. UV-Vis spectrum of the complex C_H (1.07 × 10 ⁻⁴ M in toluene; ε ₄₇₀ = 2804 L mol ⁻¹ cm ⁻¹)....	21
Figure S22. UV-Vis spectrum of the complex C_{Cum} (1.07 × 10 ⁻⁴ M in toluene; ε ₅₈₅ = 7188 L mol ⁻¹ cm ⁻¹).22	
References.	1

NMR Characterization.

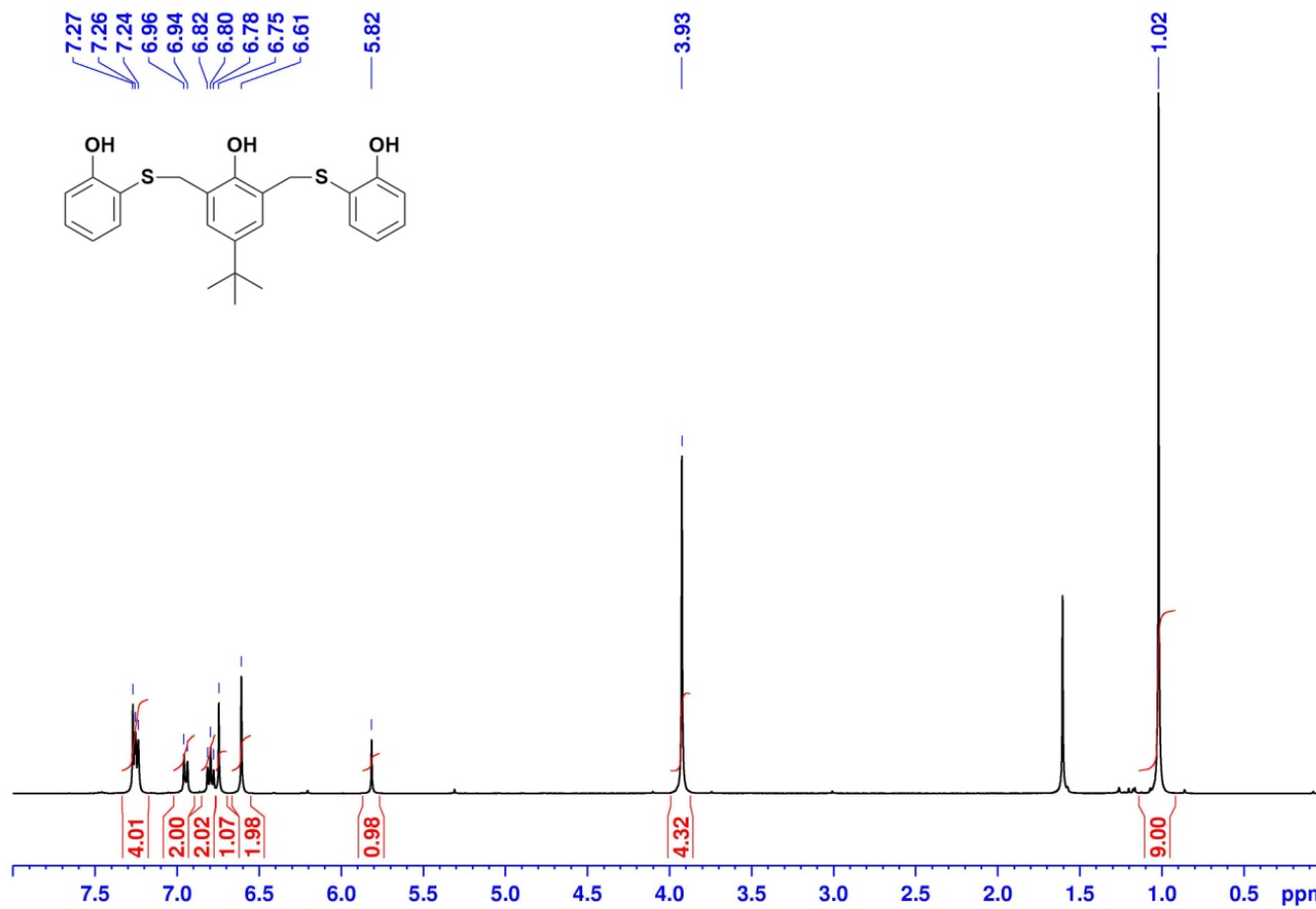


Figure S1. ^1H NMR spectrum of the pro-ligand \mathbf{L}_H (CD_2Cl_2 , 400 MHz).

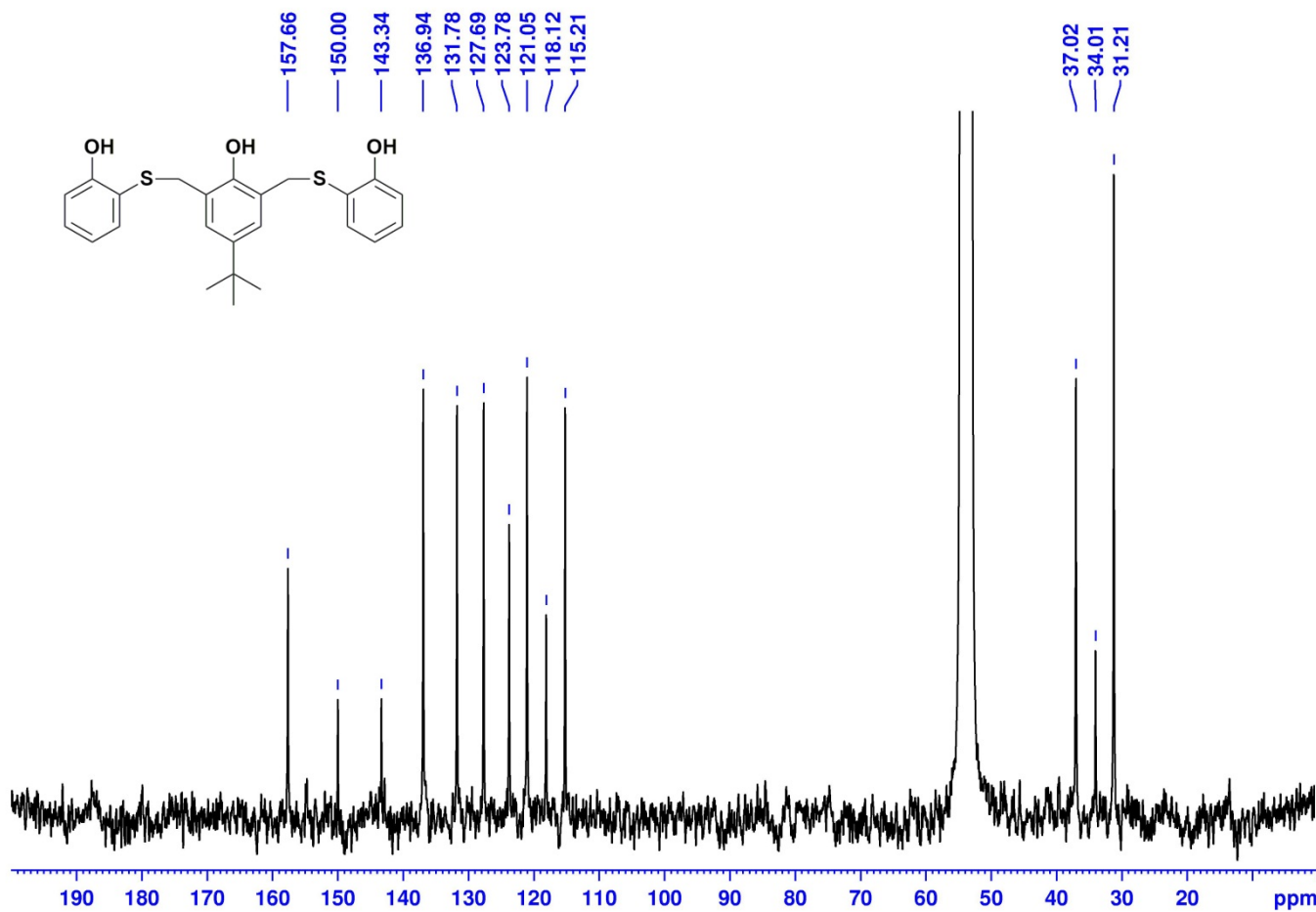


Figure S2. ¹³C NMR spectrum of the pro-ligand \mathbf{L}_H (CD_2Cl_2 , 250 MHz).

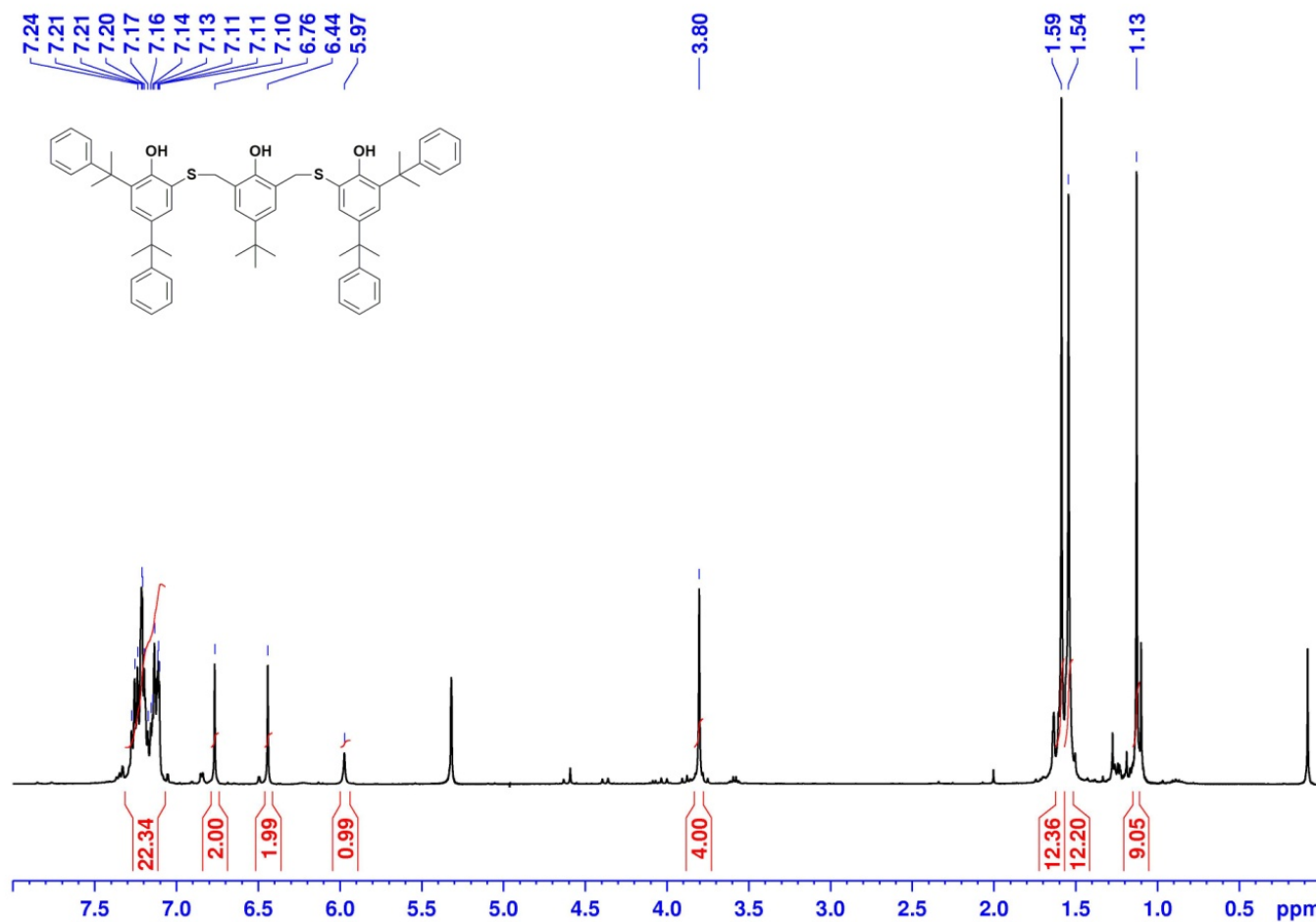


Figure S3. ¹H NMR spectrum of the pro-ligand **L_{cum}**(CD₂Cl₂, 400 MHz).

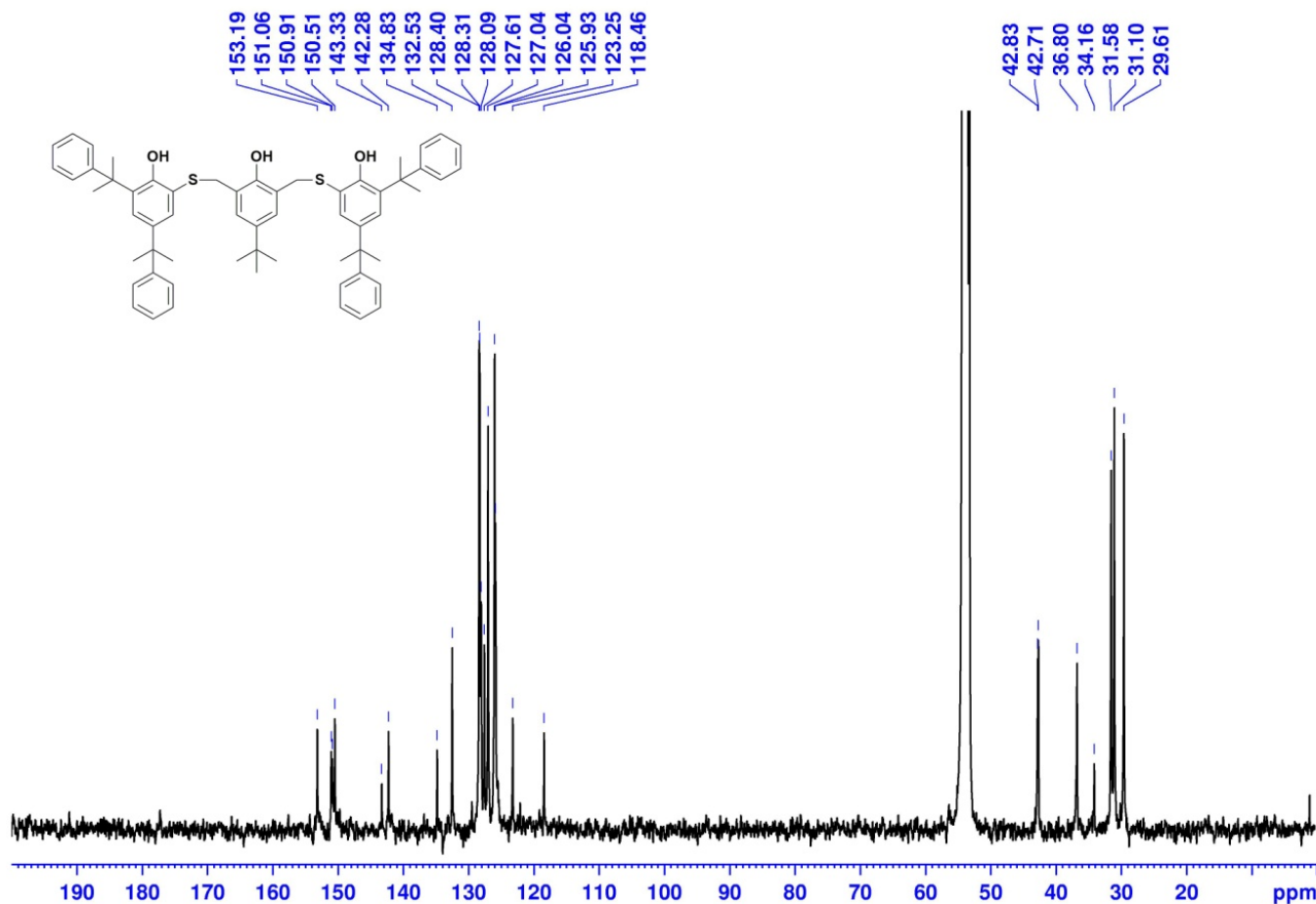


Figure S4. ¹³C NMR spectrum of the pro-ligand **L_{Cum}** (CD_2Cl_2 , 400 MHz).

ESI-MS Characterization.

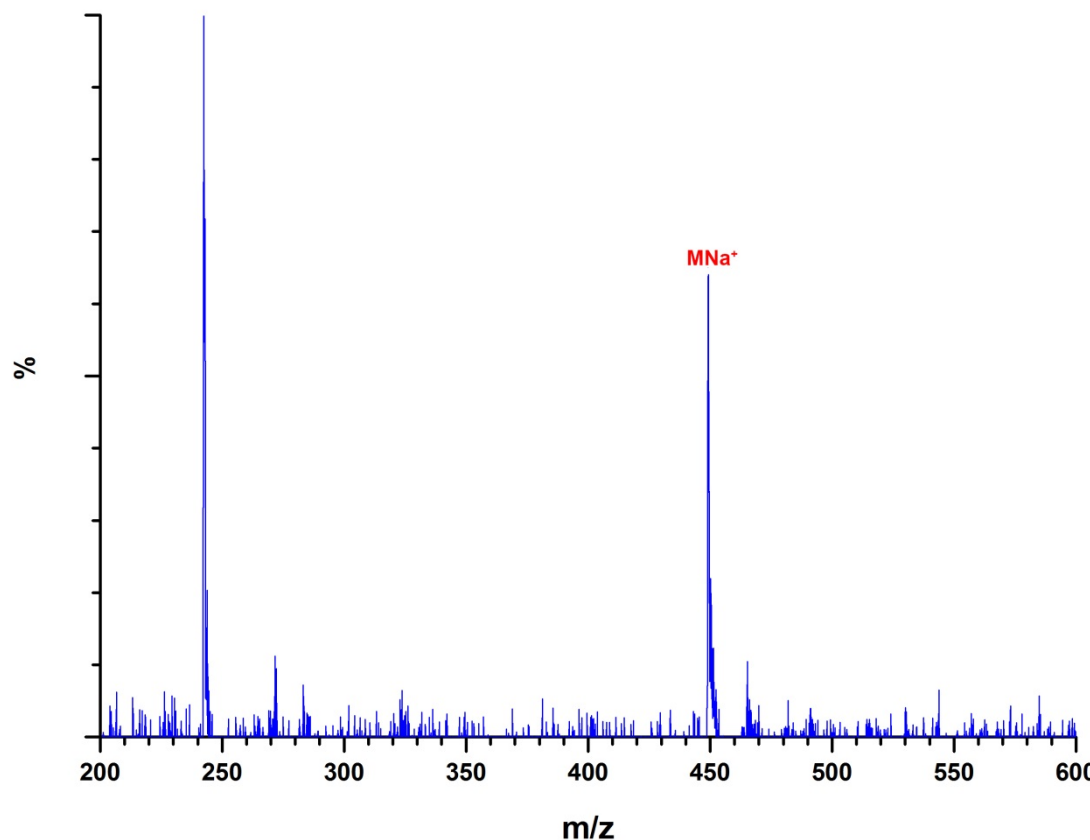


Figure S5. Mass spectrum of the pro-ligand \mathbf{L}_H (acetonitrile as solvent).

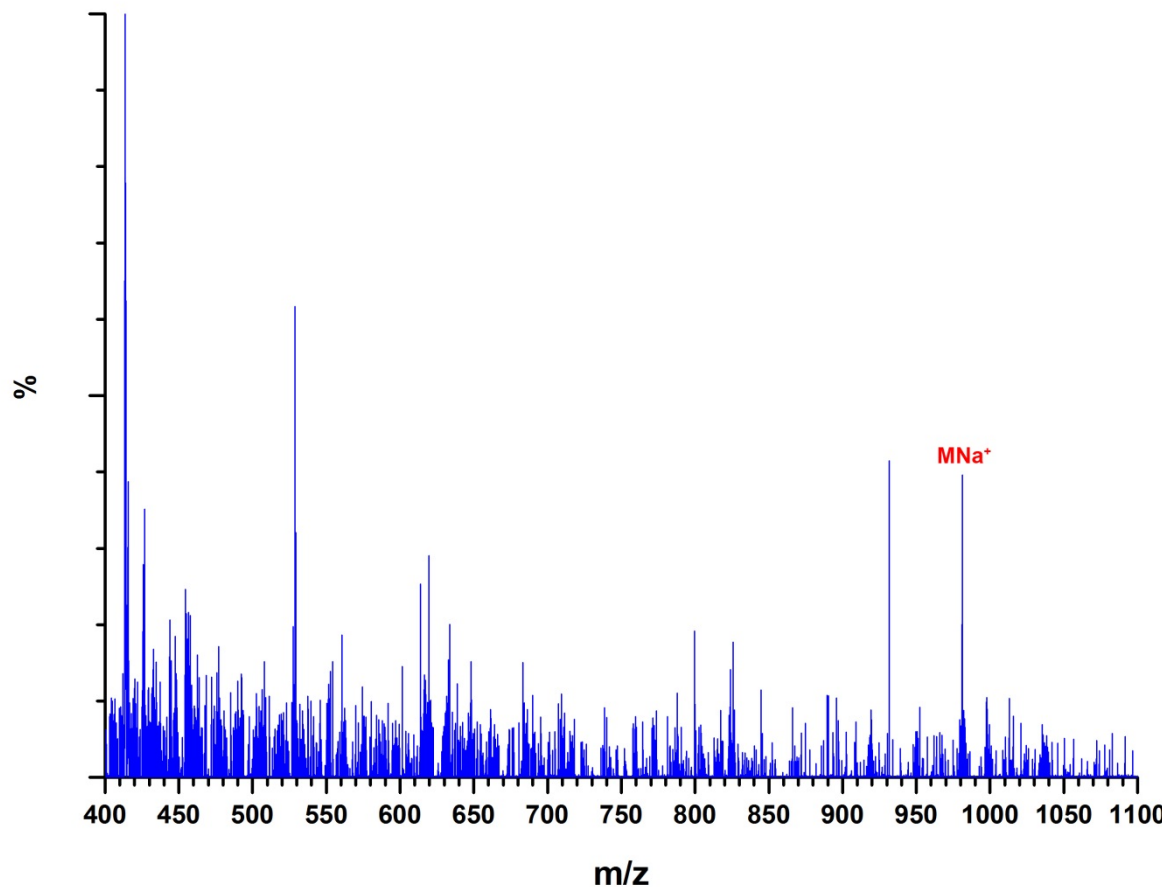


Figure S6. Mass spectrum of the complex \mathbf{C}_H (acetonitrile as solvent).

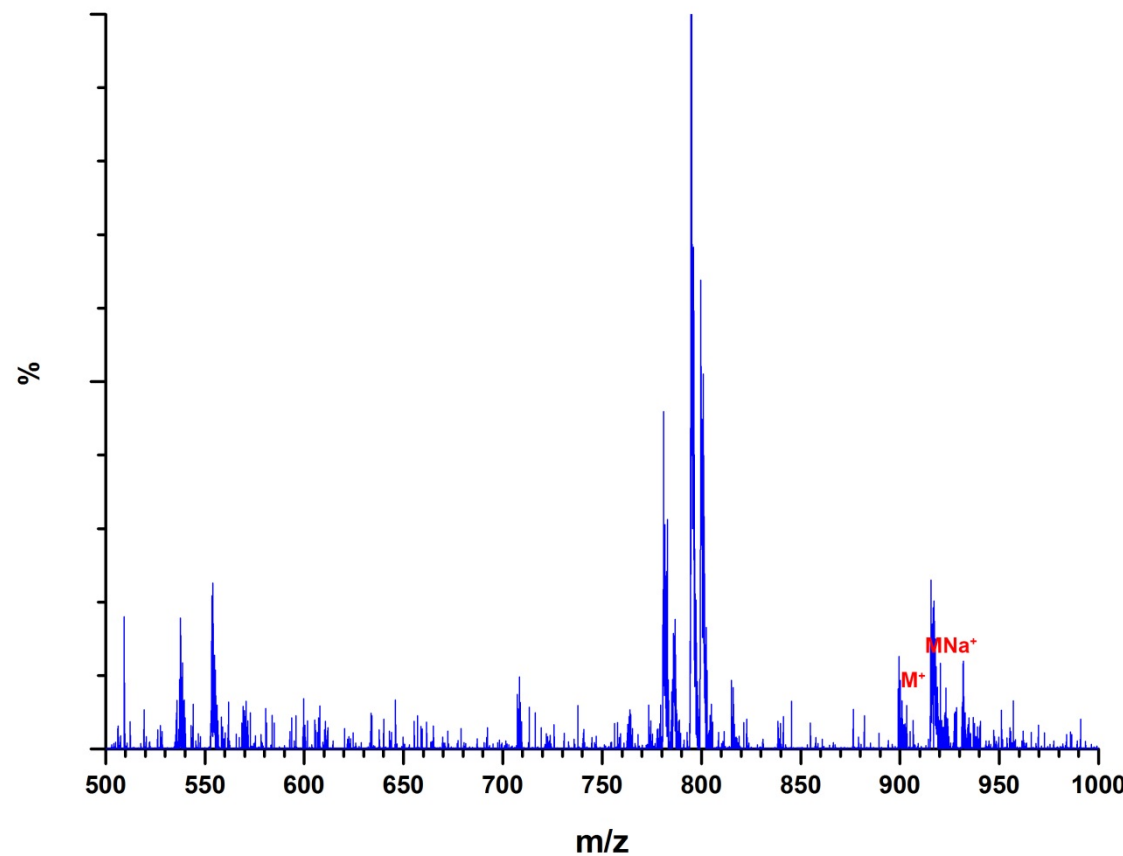


Figure S7. Mass spectrum of the pro-ligand \mathbf{L}_{Cum} (acetonitrile as solvent).

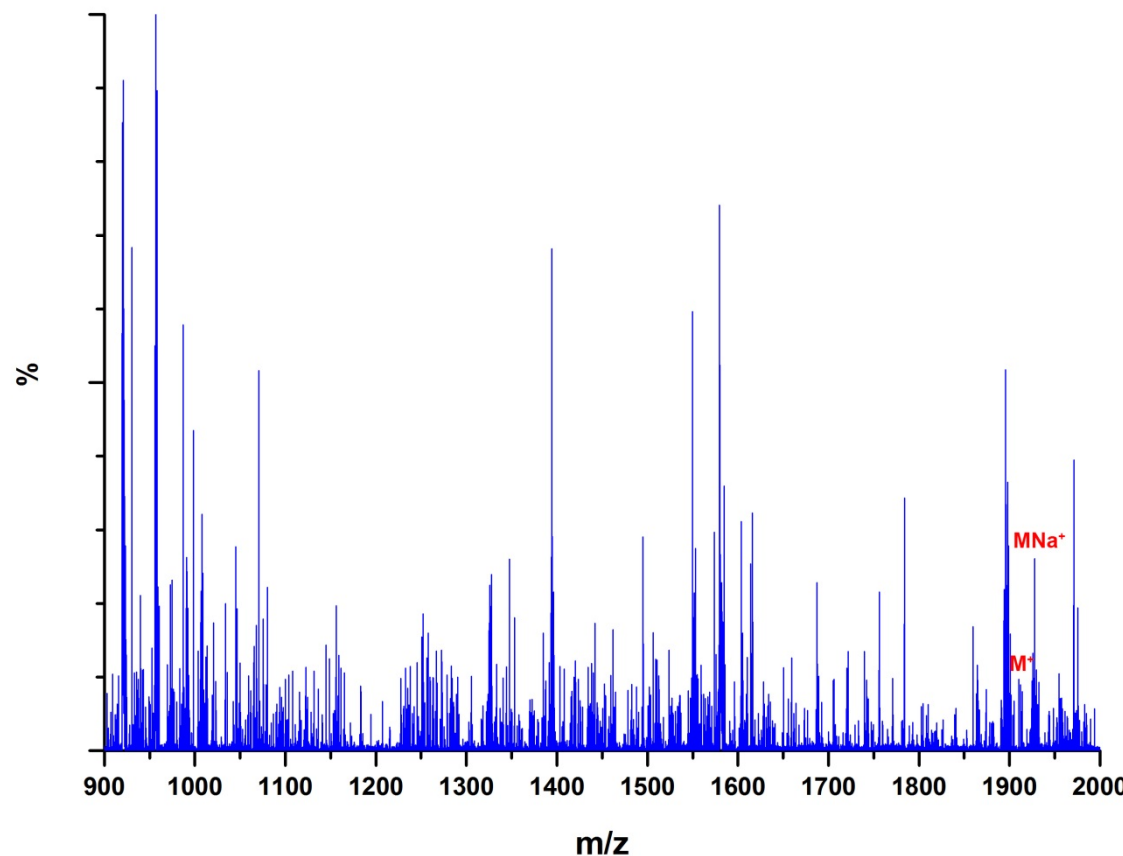


Figure S8. Mass spectrum of the complex C_{cum} (acetonitrile as solvent).

FT-IR Characterization.

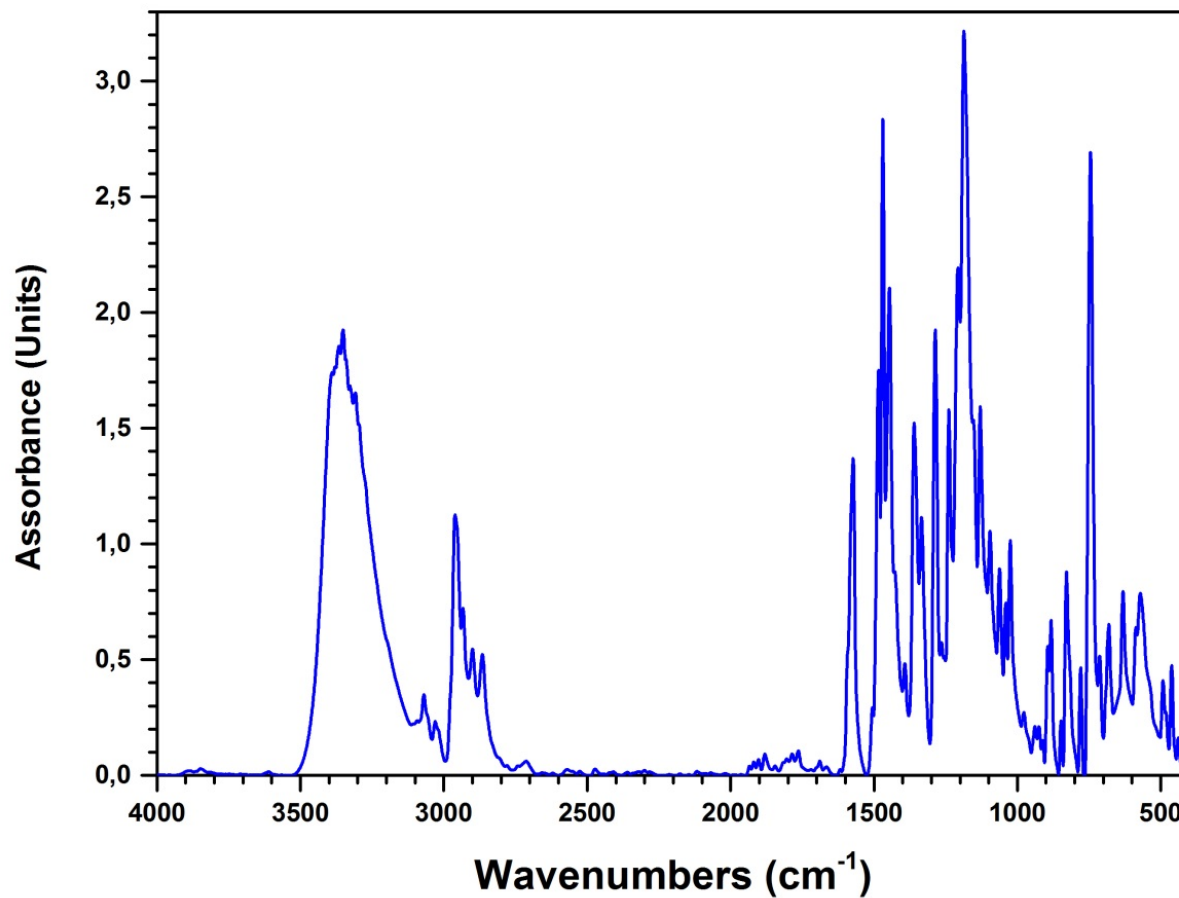


Figure S9. FT-IR spectrum of the pro-ligand \mathbf{L}_H (KBr disk).

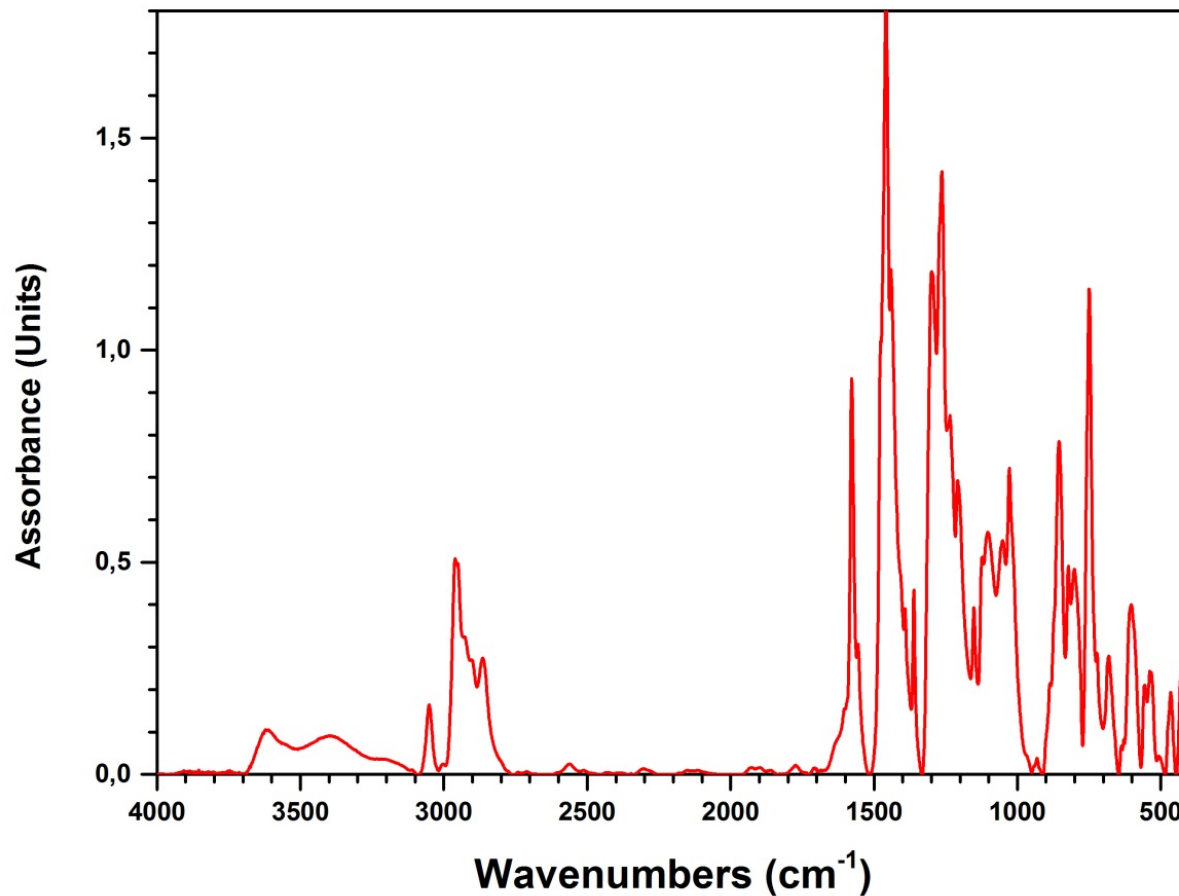


Figure S10. FT-IR spectrum of the complex \mathbf{C}_H (KBr disk).

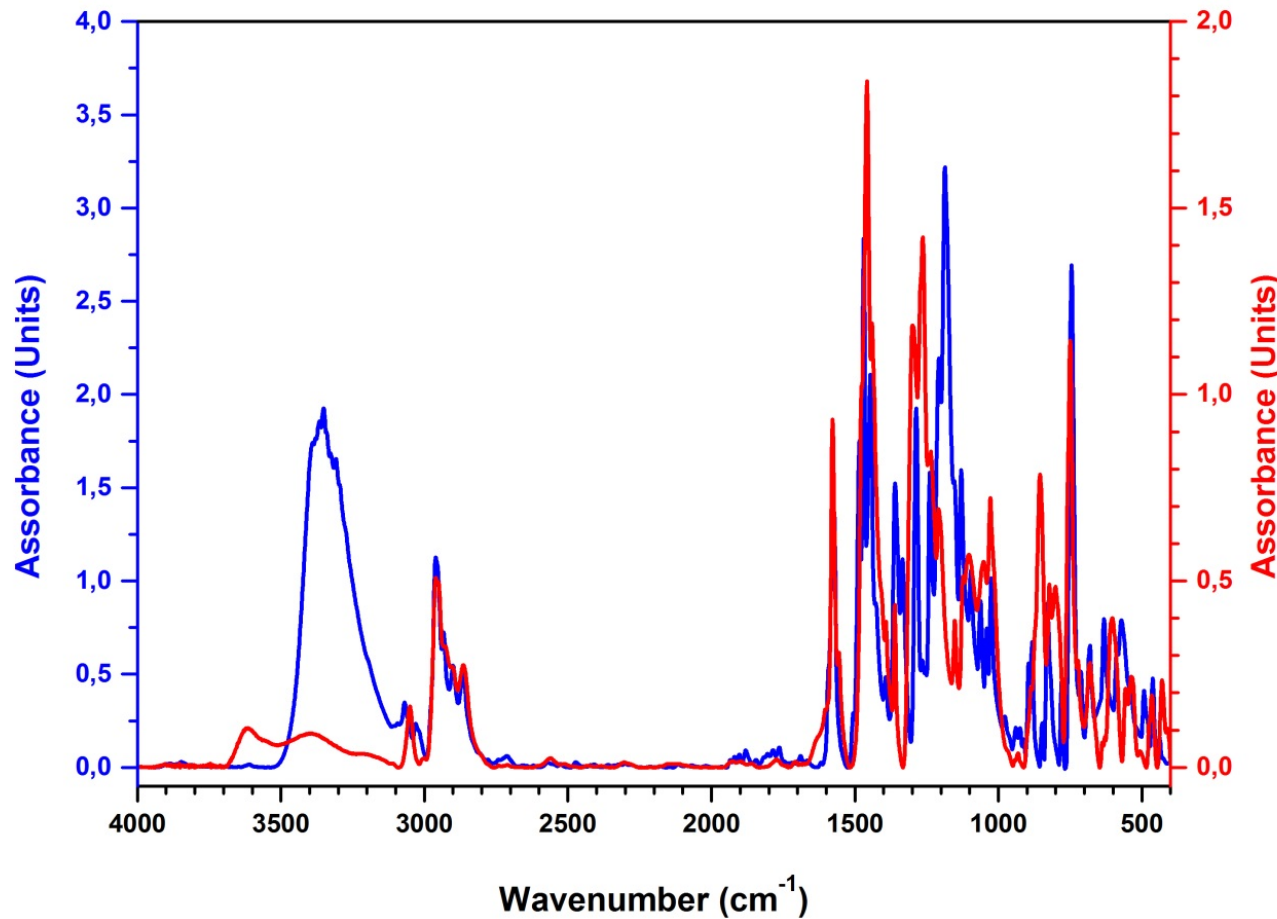


Figure S11. Comparison of the FT-IR spectra of the pro-ligand L_H (blue curve) and of the iron(III) complex C_H (red curve).

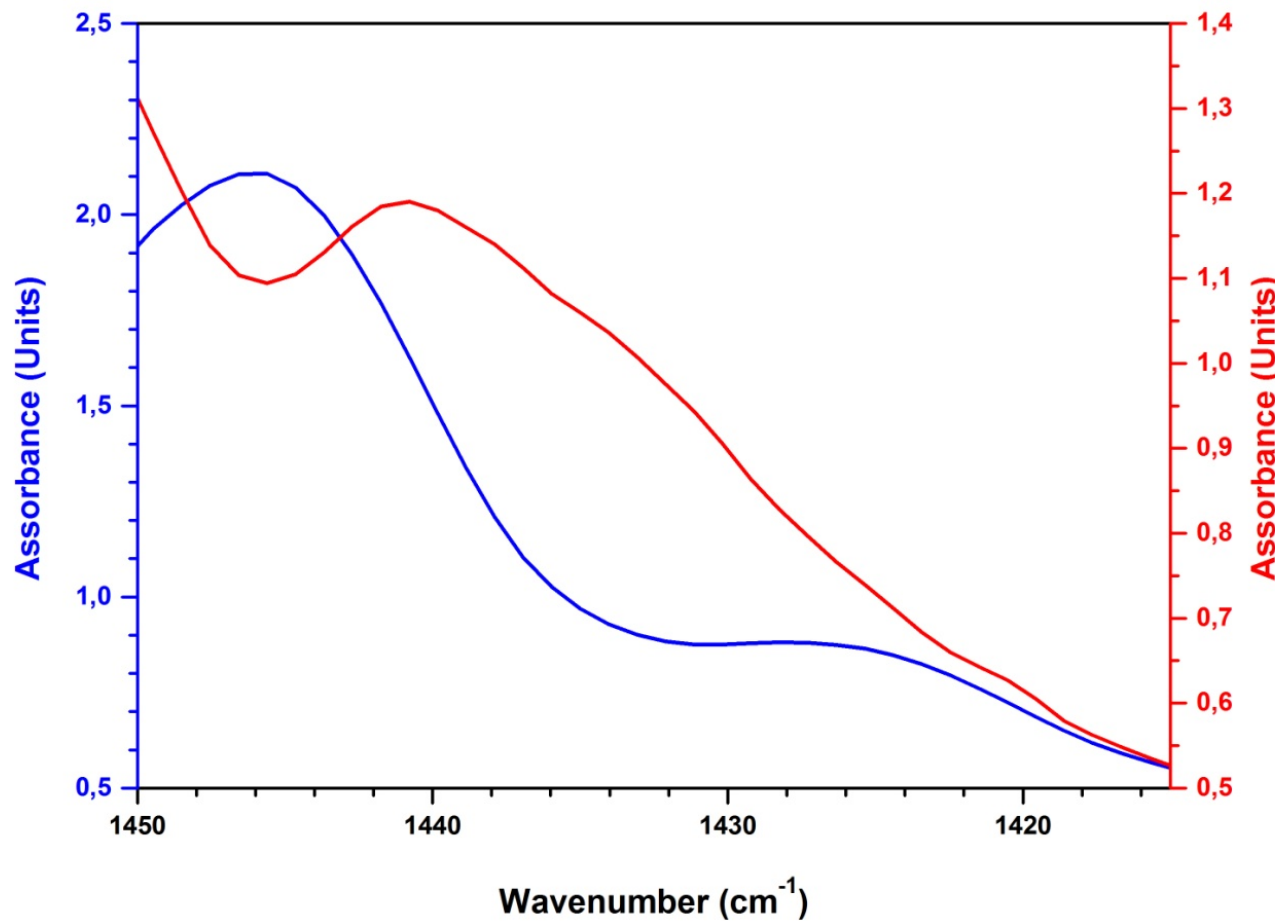


Figure S12. Magnification of the region 1450-1415 cm^{-1} (for the $\text{CH}_2\text{-S-C}$ deformation)^{1,2} of the FT-IR spectra of the pro-ligand \mathbf{L}_H (blue curve) and of the iron(III) complex \mathbf{C}_H (red curve).

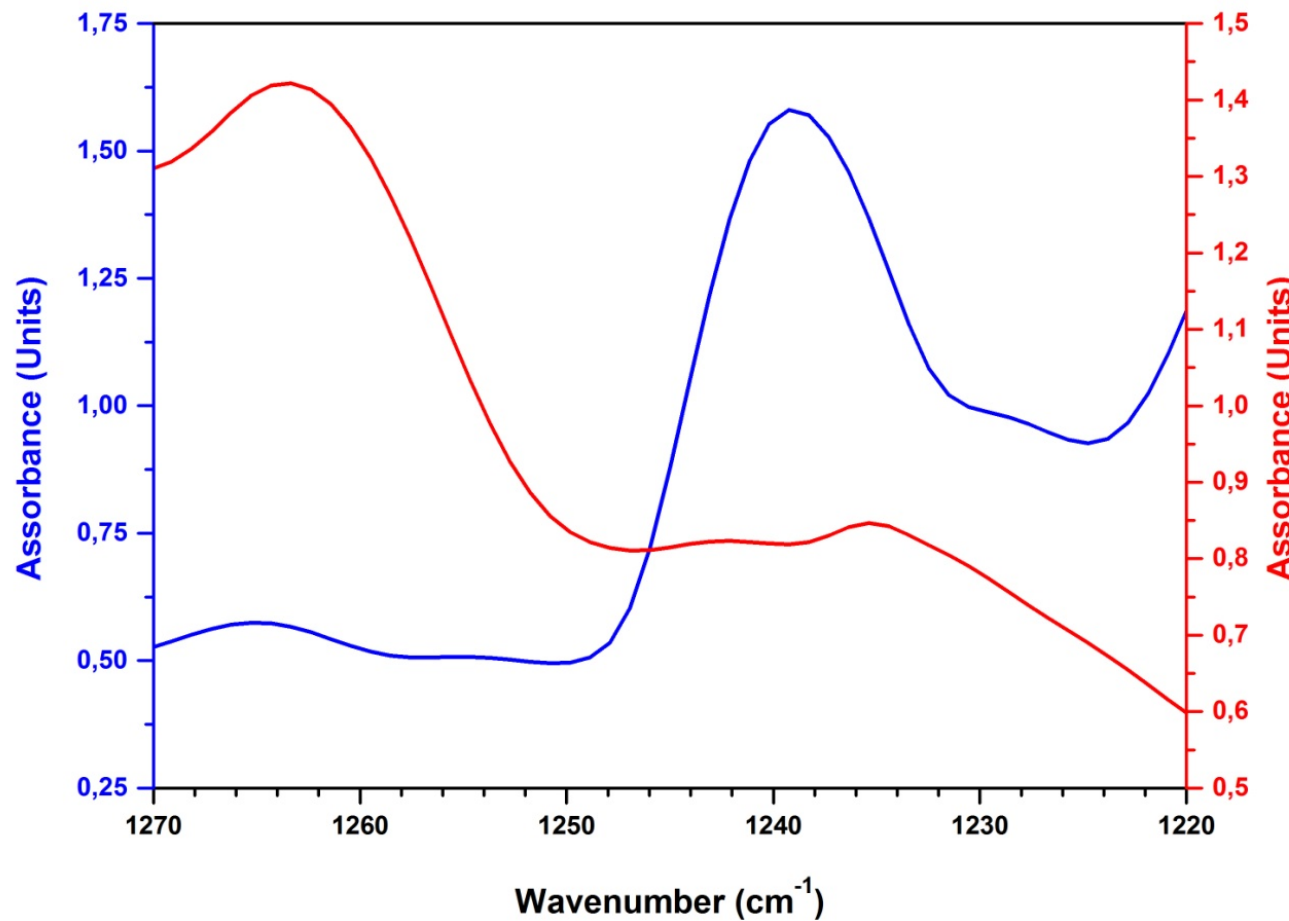


Figure S13. Magnification of the region 1270–1220 cm^{-1} (for the $\text{CH}_2\text{-S-C}$ wagging)^{1,2} of the FT-IR spectra of the pro-ligand \mathbf{L}_H (blue curve) and of the iron(III) complex \mathbf{C}_H (red curve).

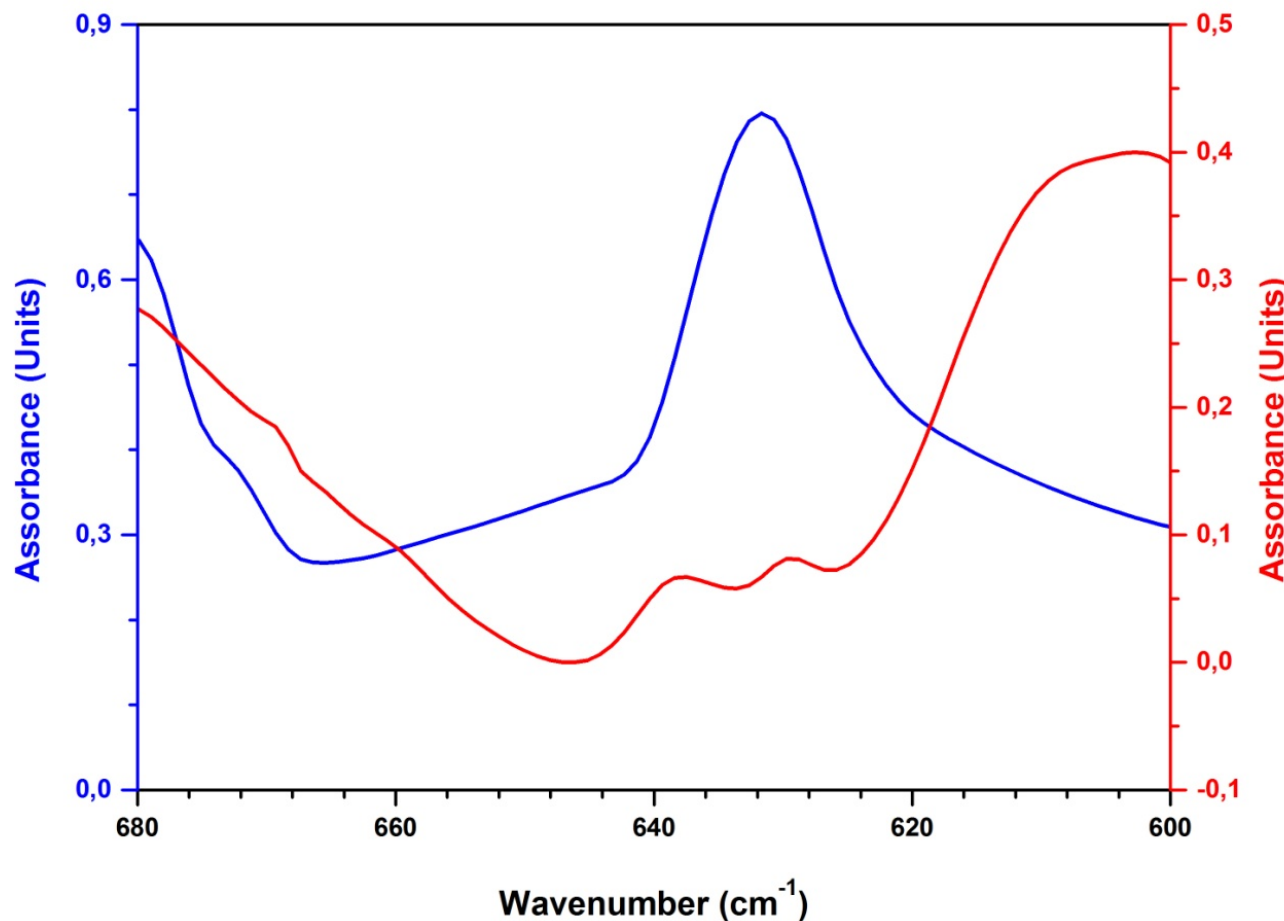


Figure S14. Magnification of the region 680-600 cm⁻¹ (for the C-S stretching vibration)^{1,2} of the FT-IR spectra of the pro-ligand L_H (blue curve) and of the iron(III) complex C_H (red curve).

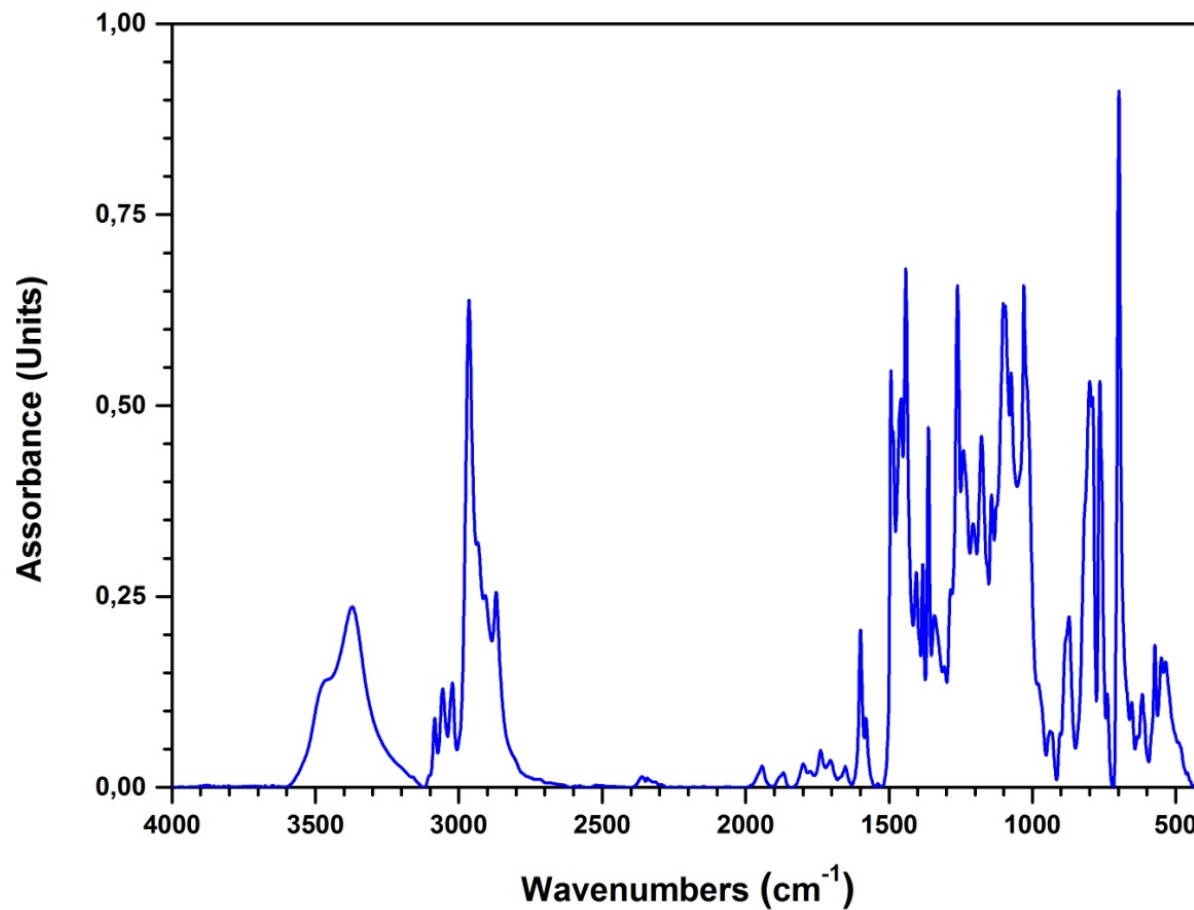


Figure S15. FT-IR spectrum of the pro-ligand \mathbf{L}_{Cum} (KBr disk).

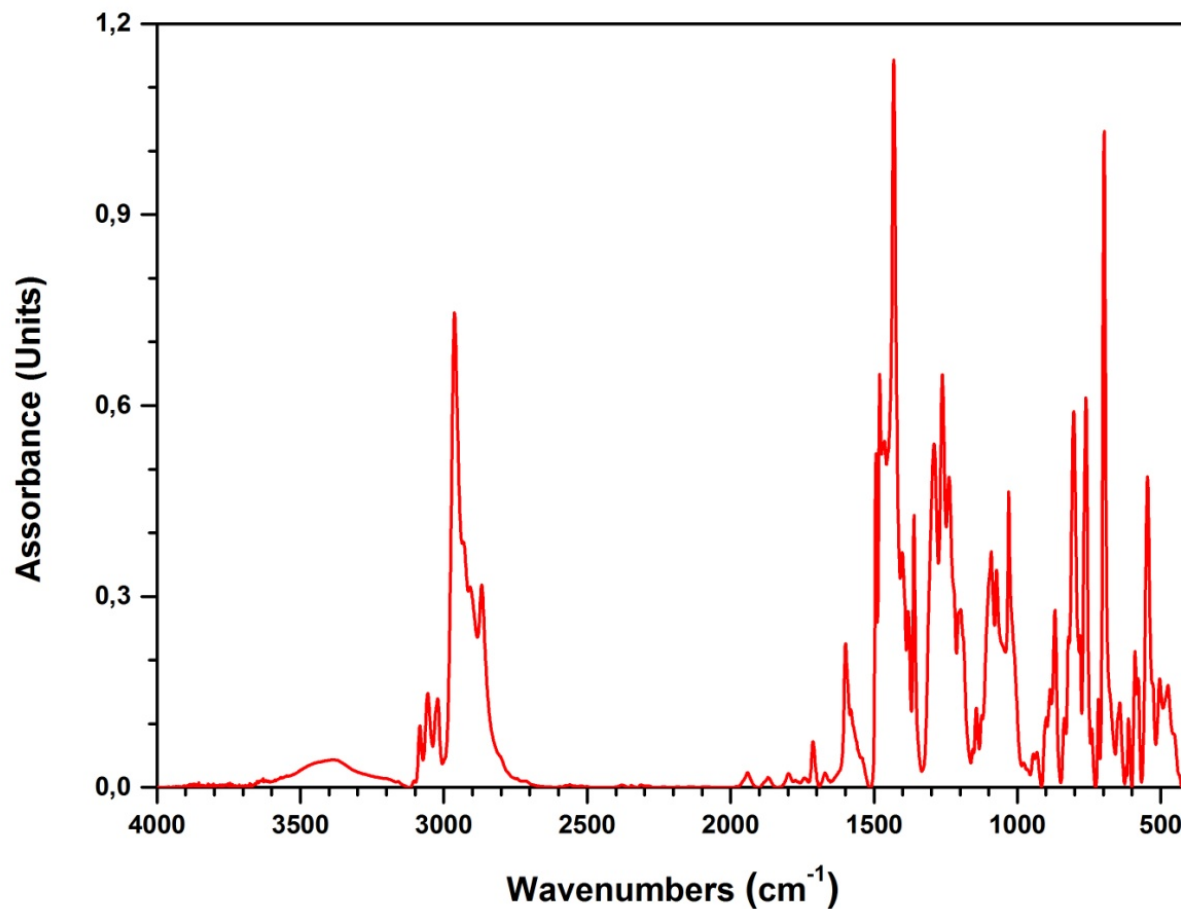


Figure S16. FT-IR spectrum of the complex \mathbf{C}_{cum} (KBr disk).

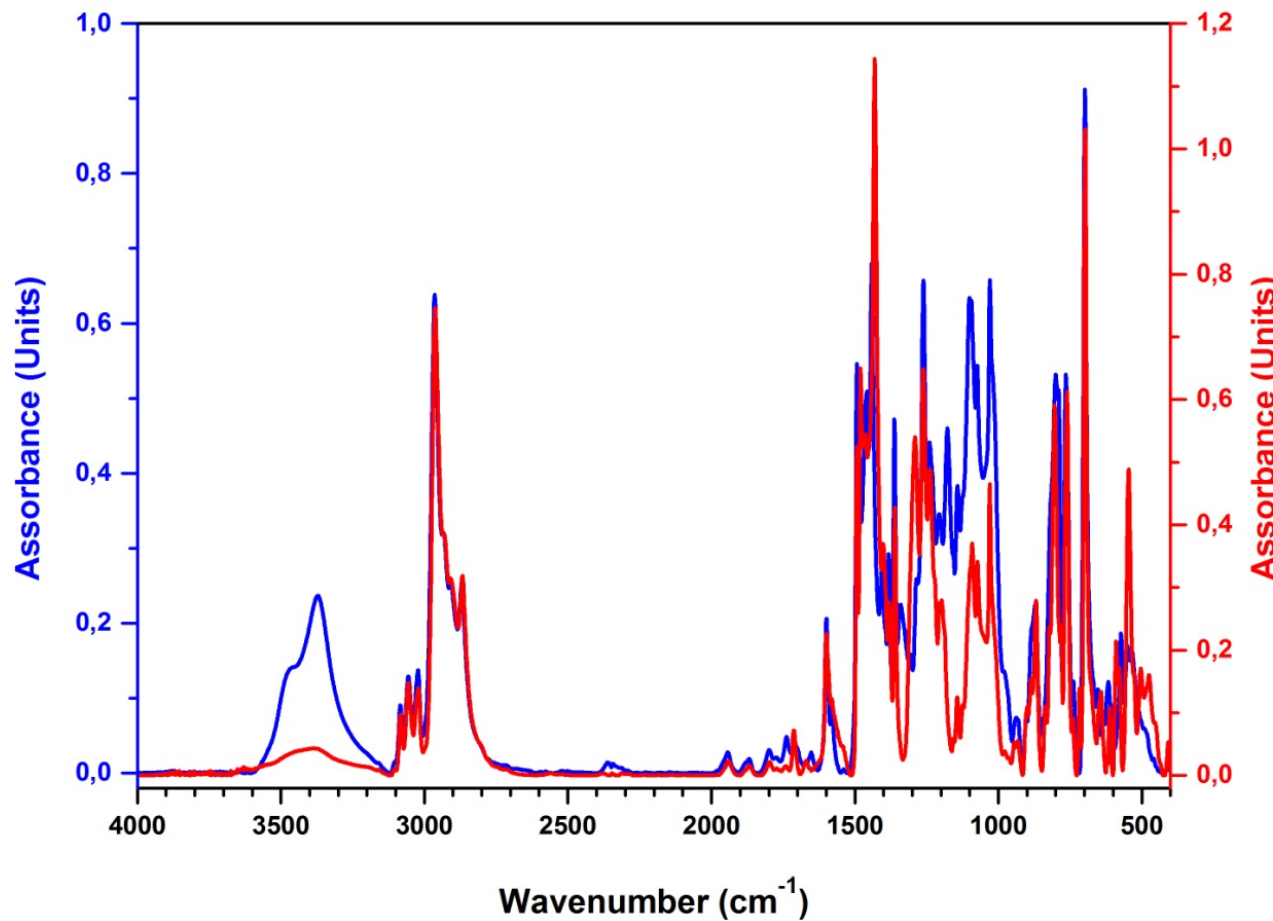


Figure S17. Comparison of the FT-IR spectra of the pro-ligand **L_{Cum}** (blue curve) and of the iron(III) complex **C_{Cum}** (red curve).

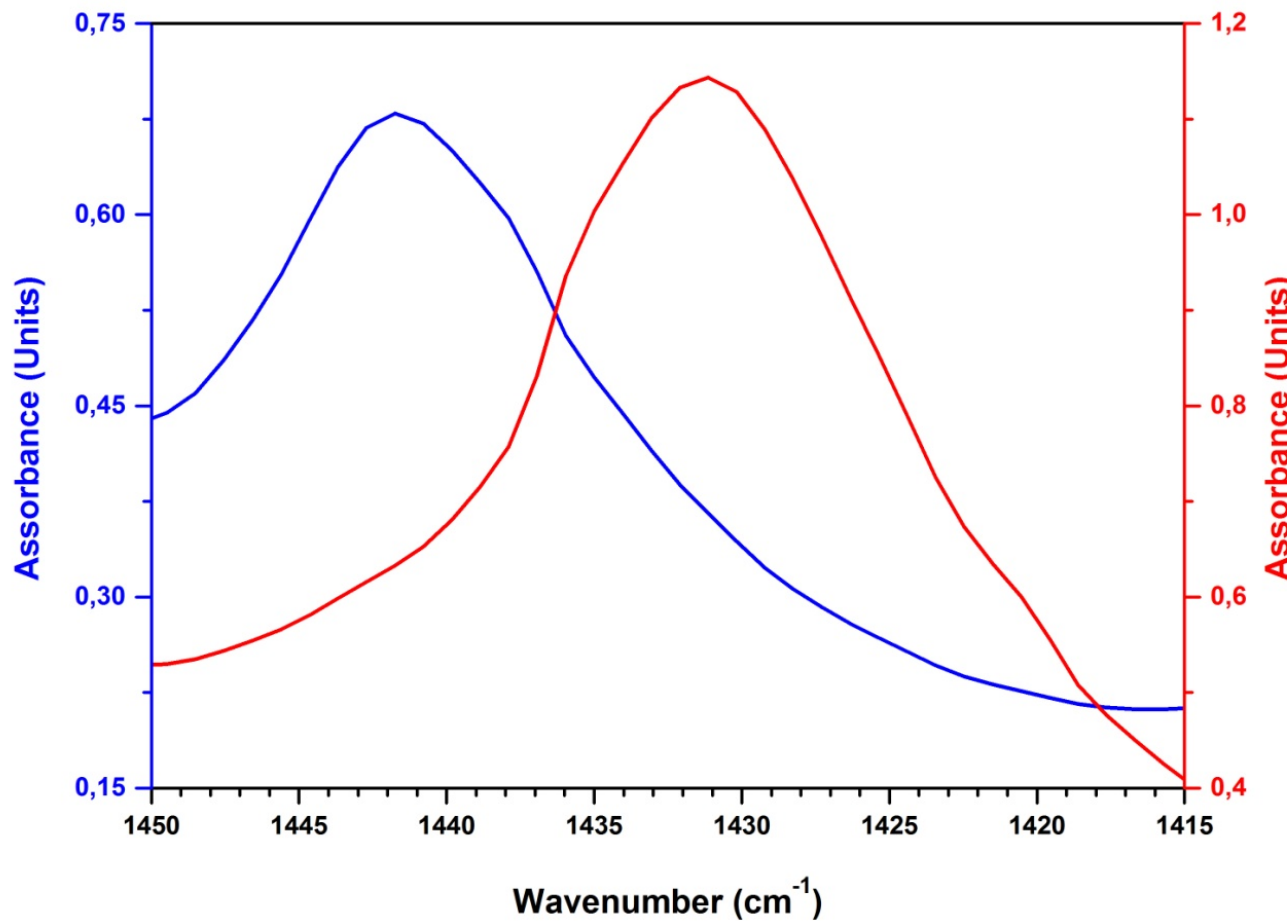


Figure S18. Magnification of the region 1450–1415 cm^{-1} (for the $\text{CH}_2\text{-S-C}$ deformation)^{1,2} of the FT-IR spectra of the pro-ligand \mathbf{L}_{Cum} (blue curve) and of the iron(III) complex \mathbf{C}_{Cum} (red curve).

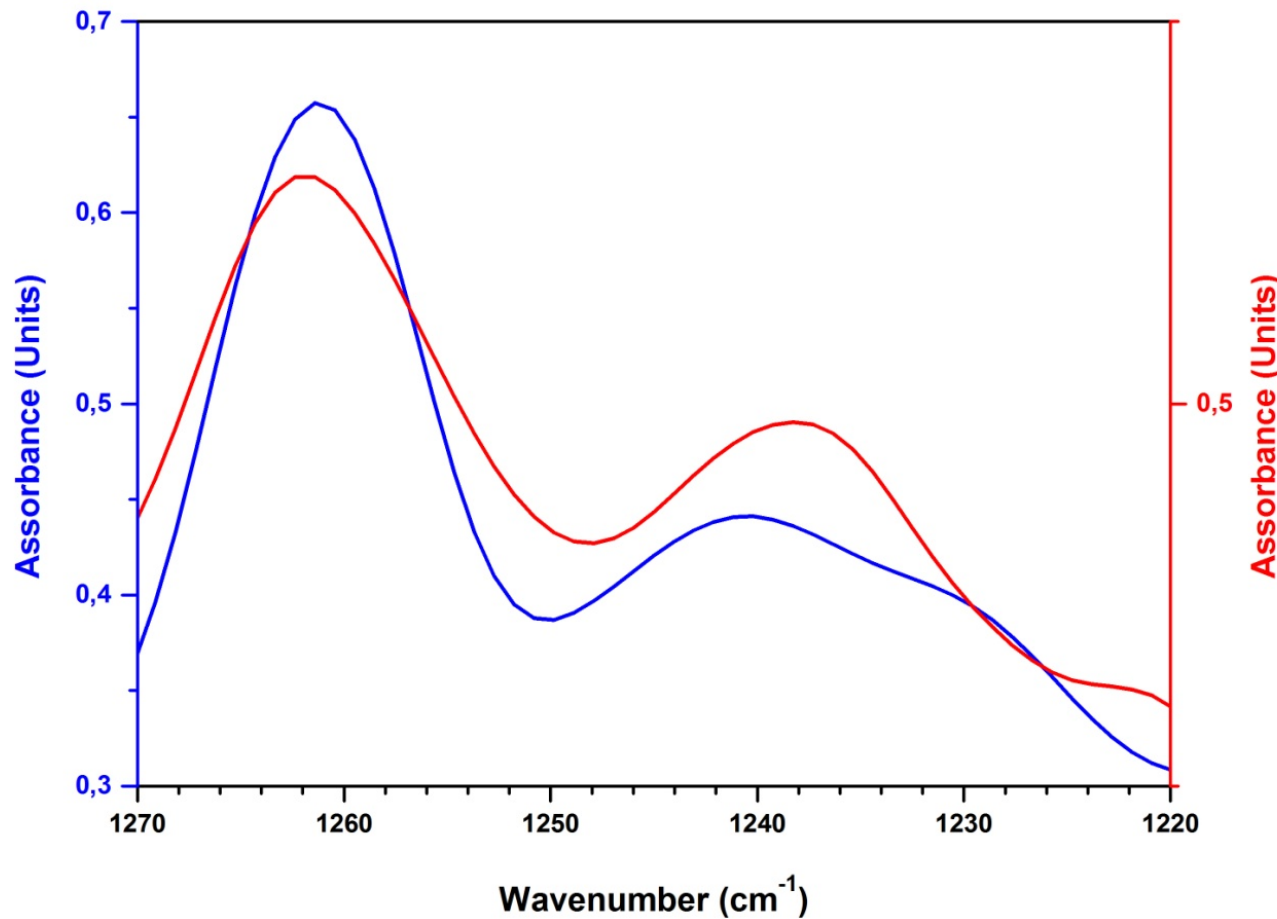


Figure S19. Magnification of the region 1270-1220 cm^{-1} (for the $\text{CH}_2\text{-S-C}$ wagging)^{1,2} of the FT-IR spectra of the pro-ligand \mathbf{L}_{Cum} (blue curve) and of the iron(III) complex \mathbf{C}_{Cum} (red curve).

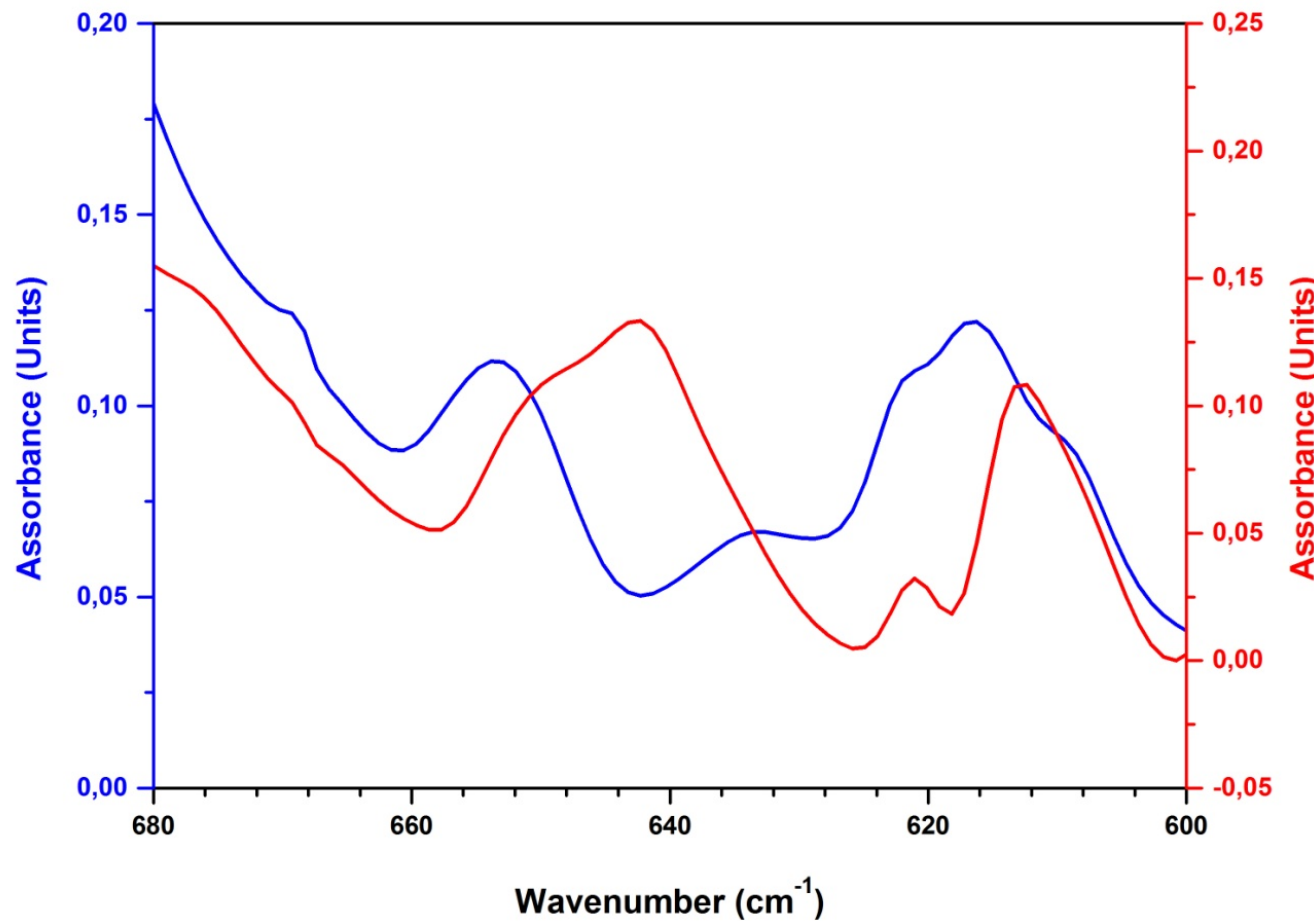


Figure S20. Magnification of the region 680–600 cm⁻¹ (for the C-S stretching vibration)^{1,2} of the FT-IR spectra of the pro-ligand **L_{Cum}** (blue curve) and of the iron(III) complex **C_{Cum}** (red curve).

UV-Vis Analysis.

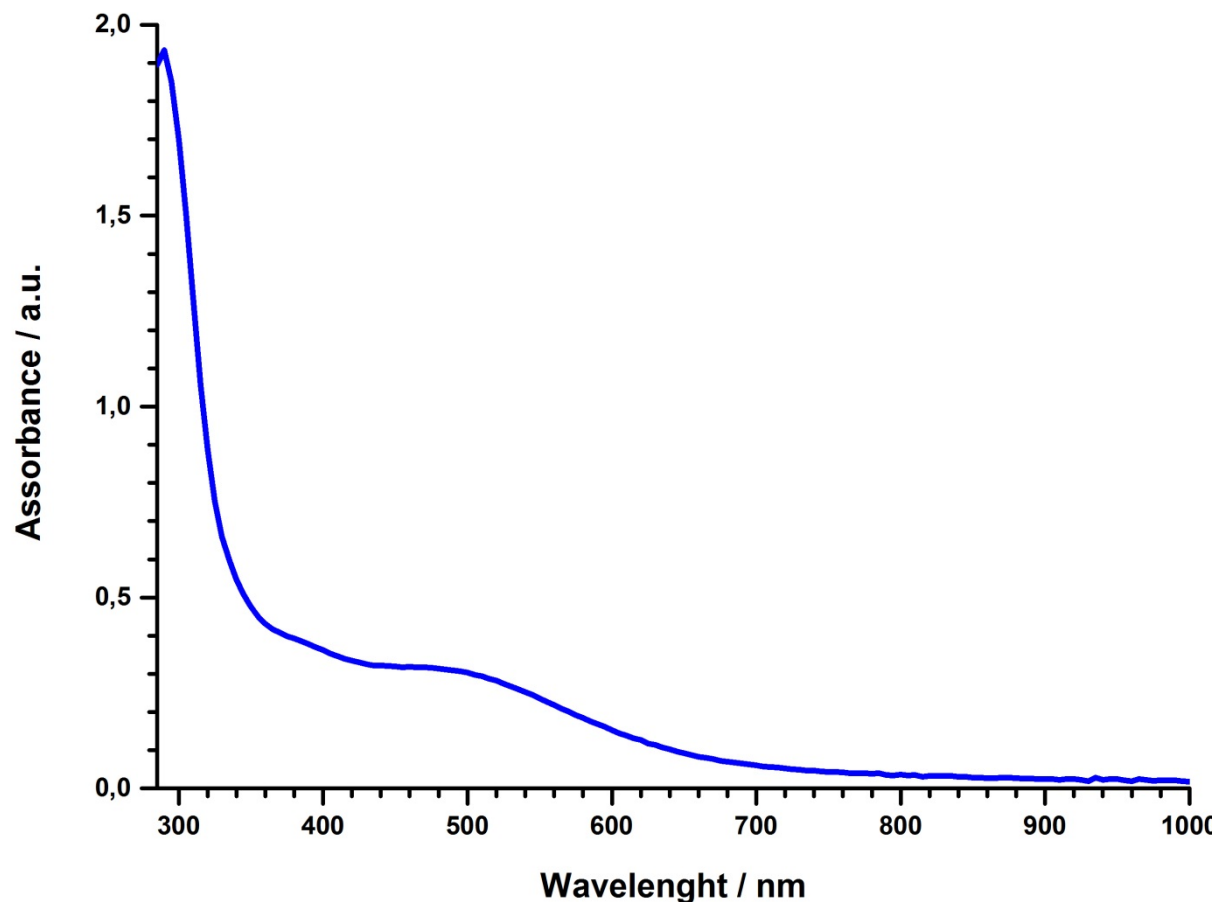


Figure S21. UV-Vis spectrum of the complex \mathbf{C}_H (1.07×10^{-4} M in toluene; $\epsilon_{470} = 2804 \text{ L mol}^{-1} \text{ cm}^{-1}$).

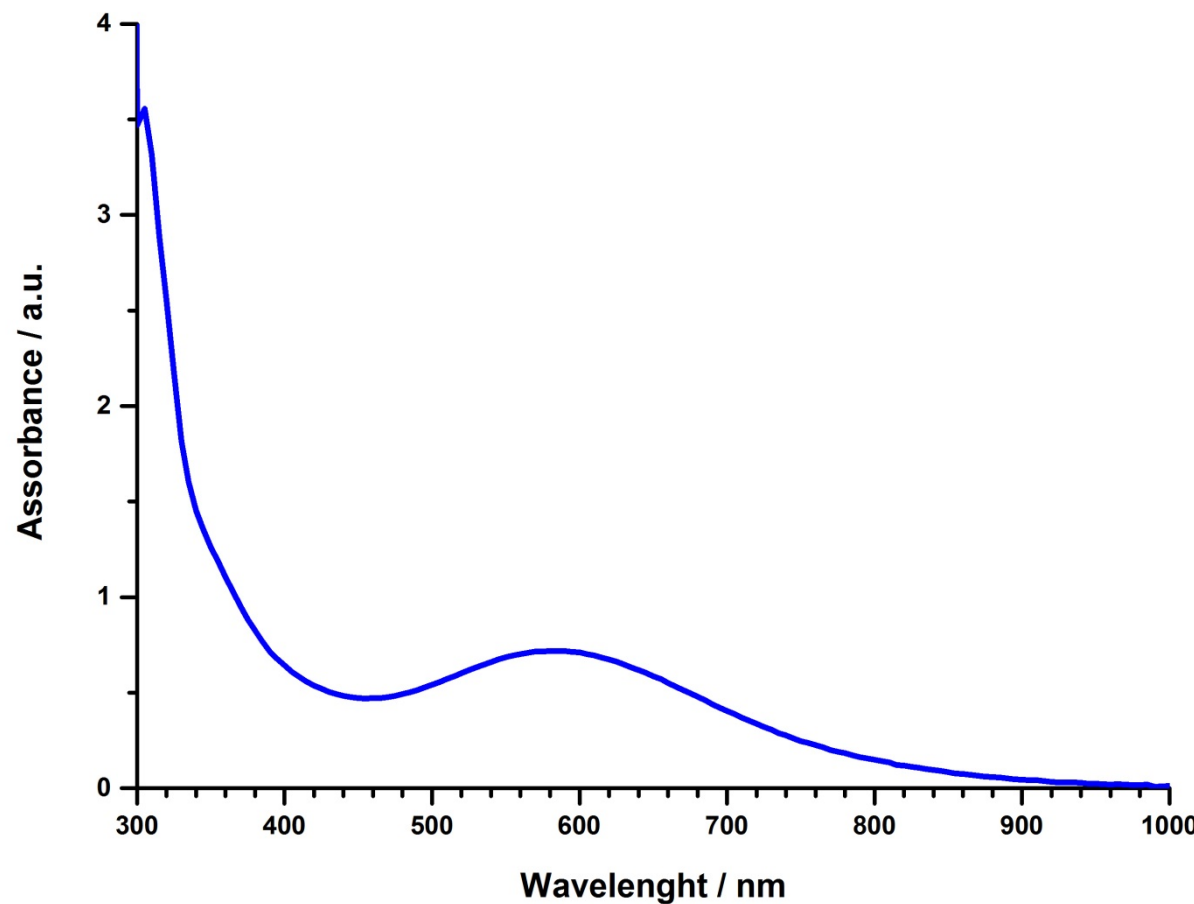


Figure S22. UV-Vis spectrum of the complex \mathbf{C}_{Cum} (1.07×10^{-4} M in toluene; $\varepsilon_{585} = 7188 \text{ L mol}^{-1} \text{ cm}^{-1}$).

References.

1. *The Sadler handbook of infrared spectra*. ed. W. W. Simons, Sadler Research Laboratories, Philadelphia, 1978.
2. *Interpreting Infrared, Raman, and Nuclear Magnetic Resonance Spectra*, ed. R. A. Nyquist, Academic Press, San Diego, 2001, pp. 65-83.